Sl. No.	IIT Ropar List of Recent Publications with Abstract Coverage: October, 2024
A	**Book Chapter(s)**
1.	An overview of production of bacterial and fungal laccases and their industrial applications SK Singh, **A Sahu**, MS Rajput, N Lal - Microbial Enzymes: Production, Purification and Industrial Applications: Book Chapter, 2025 **Abstract:** Enzymes are considered biological catalysts, playing the role of catalyzing various biological reactions. Of the many enzymes, laccases are a multi-copper oxidase group of enzymes containing histidine-rich copper-binding domains. These can be obtained from many higher plants (apples, cabbage, potatoes, turnips, etc.), fungi (Ascomycetes, Basidiomycetes, Deuteromycetes, etc.), bacteria (Azospirillum , Pseudomonas , Streptomyces, etc.), and even in insects (Calliphora , Drosophila , Musca, etc.). However, industrially important laccases are extracted and processed from various bacterial and fungal species, depending upon their usage. Laccases are one of the most versatile enzymes with innumerable industrial applications. Laccases are known to be used in the pulp and paper industry as a lignin-degrading agent. Laccases are used in textile industries as a substitute for conventionally used chemicals for biostoning and toxin neutralization. These enzymes have also found substantial usage in food industries, such as the treatment of tea; baking industry to enhance the color, flavor, and texture; and in food packaging. Pharmaceutical industries are also using laccases for the synthesis of antimicrobials, anesthetics, anti-inflammatory, antibiotics, personal-care agents, etc. Laccases have also found their wide applications in the field of enzymatic treatment of many industrial wastewaters, and hence these are now extensively being explored for bioremediation purposes of industrial wastewater. Laccases have also found their applications as biosensors for the detection of phenols, polyphenols , anilines, and oxygen. The current review summarizes the structure, mode of action, sources, substrates and mediators, production as well as applications of fungal and bacterial laccases.
2.	Assessment of the failure mechanisms of URM infilled RC hill buildings **Z Naorem, P Haldar** - Developments in Structural Engineering, Volume 4: Book Chapter, 2024 **Abstract:** There is an ever-increasing demand for constructible land in the cities and towns of the Indian Himalayan region owing to the rapidly rising population in the country. Due to the scarcity of flat lands, buildings in this region are mostly constructed on sloping terrain with foundations at different levels. These types of structural configurations adversely affect the seismic performance of the buildings in a region where the seismicity is generally extremely high. The problem is further complicated by the fact that proper earthquake resistant design guidelines as per Indian Standards are unavailable for buildings constructed in hilly terrain. The seismic response of such buildings varies depending on the type of structural configuration and gets complicated when we consider the complex interaction between frame and Un-Reinforced Masonry (URM) infills. The aim of the manuscript is to achieve a comprehensive understanding of URM infilled Reinforced Concrete (RC) hill buildings considering various structural configurations that are common in hilly region. Towards this purpose, an analytical study has been undertaken on a set of URM infilled RC buildings having the most commonly found structural configurations in hilly region. Seismic response is evaluated with the help of non-linear time history analyses. It has been observed that the response parameters in terms of Inter-storey Drift Ratio (IDR) and roof acceleration were higher for buildings with setbacks in the structural configuration. Consequently, the extent of damage probability is also higher for setback

	buildings. It has also been observed that collapse of all the considered buildings is caused predominantly by shear failure of short columns.
3.	Biomedical applications of biogenic carbon-based fluorescent nanoparticles **K Kaur, G Singh**, R Badru, N Kaur, **N Singh** - Biogenic Nanomaterial for Health and Environment: Book Chapter, 2024 **Abstract:** The wide-ranging applications of carbon dots (CDs), which can be developed using either green or chemical precursors, have been made possible due to their reported properties and the various precursors that have been identified. This has opened up new opportunities for the development of high-quality CDs and their use in optoelectronic devices, bioimaging, and other applications. Green precursors can be derived from fruits, vegetables, flowers, leaves, seeds, stems, crop residues, fungi/bacteria species, and waste products, while chemical precursors can be categorized as either acid reagents or non-acid reagents. It provides a brief review of the past ten years of CD synthesis using both green and chemical precursors, as well as the use of CDs as sensing materials in biomedical applications. This comprehensive review will be a valuable resource for researchers who are interested in synthesizing high-quality CDs for a variety of applications.
4.	Community-level solar thermal systems **V Bhalla**, V Khullar, **H Tyagi** - Wind and Solar Based Energy Systems for Communities: Book Chapter, 2024 **Abstract:** This chapter provides a brief background in the various conventional methods (surface-based absorption of solar energy) available for harnessing solar thermal energy at a community level. It describes some of the main differences between the typical non-concentrating as well as concentrating type solar collectors, and highlights some of their main attributes. It also presents in detail the results of a novel technique for harnessing solar energy. In this technique, the solar energy is directly absorbed by the fluid (volumetrically) using nanoparticle-laden fluids (hence, it is categorized as volumetric-based absorption of solar energy). Such a collector is analysed in detail using a numerical model. The results of the numerical model are then discussed, which simulates the requirements of hot water for a typical community consists of about 10 households (40 persons). Two of the main performance evaluation parameters - collector efficiency and the fluid outlet temperature - have been extensively studied, and the influence of various design and operational parameters (particle volume fraction, mass flow rate, solar irradiation, collector height, collector length) on these two have been studied in detail. Moreover, the variation of spectral intensity, energy generation rate and spatial temperature distribution within the collector has been quantified. The calculations also show the dimensions of the desired solar collector in order to meet the daily hot water requirements (100 kg/person) for this community.
5.	Strategies and implementation for achieving sustainable flood risk management **NG Paswan, S Pathak** - Sustainable Development and Geospatial Technology: Volume 2: Applications and Future Directions: Book Chapter, 2024 **Abstract:** Flood is considered one of the most destructive and catastrophic phenomena among all-natural calamities. Flood risk is a function and a product of hazard and vulnerability. The selection of appropriate flood management strategies necessitates a thorough understanding of the risk mechanism. Flood Risk Management (FRM) approaches are critical for reducing the devastating effects floods can have on human health, economy and the environment. FRM comprises a variety of tactics and approaches for mitigating these impacts, whether on a local or a global basis. FRM employs a systematic strategy that has proven critical for mitigating flood-related risks. This chapter examines various FRM approaches, analysing their limitations, characteristics and key components. Furthermore, the chapter discusses the importance of remote

	sensing and Geographic Information Systems (GISs) in supporting FRM activities. Using these tools, stakeholders, urban planners and watershed managers can better forecast and minimise the effects of floods through proactive actions.
B	**Conference Proceeding(s)**
6.	A further study on weak byzantine gathering of mobile agents **A Saxena, K Mondal** - Proceedings of the 25th International Conference on Distributed Computing and Networking, 2024 **Abstract:** The gathering of mobile agents in the presence of Byzantine faults is first studied by Dieudonné et al. Authors provide a polynomial time algorithm handling any number of weak Byzantine agents in the presence of at least one good agent considering start-up delays, i.e., the good agents may not wake up at the same time. Hirose et al. come up with an algorithm considering start-up delays that use a strong team of at least 4f2 + 8f + 4 many good agents but runs much faster than that of Dieudonné et al. Later Hirose et al. provide another polynomial time algorithm for gathering in the presence of at least 8f + 8 good agents. However, this algorithm does not work in the presence of start-up delays, also simultaneous termination of good agents is not possible. We, in this work, provide an algorithm considering start-up delays of the good agents reducing the number of good agents w.r.t. Hirose et al. from 4f2 + 8f + 4 to f2 + 4f + 9. Also, our algorithm guarantees simultaneous termination of the good agents.
7.	Attentive A* for visual cue based path planning in complex environments **A Kumar, K Verma, A Garg, SS Jha** - Agents and Robots for reliable Engineered Autonomy (AREA 2024), 2024 **Abstract:** Navigating through complex environments has always been a big challenge for smart robots and AI agents. This paper focuses on a specific problem within the domain of path planning, aiming to aid agents in navigating through intricate environments using raw images as input. Data-driven path-planning algorithms have emerged as a cogent solution to such problems. These algorithms are a fusion of deep learning models for cost approximation, and differentiable versions of classical planning algorithms. While these methods excel at handling combinatorial data, their computational demands are high. These often leads to poor function approximation due to ineffective feature extraction in complex environments. Drawing from the significance of the attention mechanism in various deep learning applications, we present Attentive A*, introducing attention to data-driven path-planning algorithms. The proposed approach provides precise cost approximations by leveraging visual cues, resulting in enhanced performance across various metrics. A comprehensive assessment is conducted on diverse datasets, including MP, Tiled MP, CSM and Warcraft, to assess the effectiveness of the proposed approach compared to other baselines.
8.	Barker coded thermal wave imaging for defect detection of carbon fiber reinforced polymer **A Rani, J Kaur**, G Dua, **KR Sekhar**, R Mulaveesala - Advances in Non Destructive Evaluation (NDE, 2021): Conference Proceedings, 2024 **Abstract:** InfraRed Thermography (IRT) is a widely used Non-Destructive Testing (NDT) method for inspection of various structures and components in the fields of renewable energy, aerospace, automobiles industry, etc. The paper presents Barker Coded Thermal Wave Imaging (BCTWI) technique based on pulse compression approach to obtain enhanced probing depth and resolution for testing of Carbon Fiber Reinforced Polymers (CFRP) sample. The time domain and frequency domain analysis has been carried out for quantitative assessment of the defects in the CFRP sample. Results shows that BCTWI with time domain approach significantly improves the defect depth resolution in comparison to the conventional frequency domain analysis approach.

9.	Comparative analysis of infrared thermographic techniques for non-destructive testing and evaluation of materials **P Mishra, A Rani, R Sekhar**, R Mulaveesala - Advances in Non Destructive Evaluation (NDE, 2021): Conference Proceedings, 2024 **Abstract:** Among the various widely used thermographic techniques, Frequency Modulated Thermal Wave Imaging (FMTWI) has proven to be indispensable for evaluating various materials. There are growing concerns of surface and sub-surface defect detection capabilities with moderate peak power heat sources compared to the widely used conventional pulse-based thermographic methods. In average testing, time compared to the sinusoidal modulated lock-in thermography make FMTWI an invaluable technique. The present work highlights a comparative study on FMTWI technique using multi-transform analysis approaches for Non-Destructive Testing and Evaluation (NDT&E) of materials.
10.	Detection and estimation of sub-surface defects using frequency modulated thermal wave imaging G Dua, N Kaur, **A Sharma**, R Mulaveesala - Advances in Non Destructive Evaluation (NDE, 2021): Conference Proceedings, 2024 **Abstract:** Thermal wave imaging is an imperative non-destructive testing technique with inherent capabilities for testing and evaluating various solid materials. The method has the advantages of being a safe, fast, non-contact, and reliable technique, mapping surface temperature distribution which is utilized for non-destructive testing of materials. This work focuses on inspecting mild steel material, extensively used in various industries like construction, transportation, oil and gas, etc. Most commonly used industrial components made up of mild steel include construction beams, chimneys, sliding and rod type gates, etc. Safety and demand for quality of in-service products require thorough testing and reliable monitoring methodology to avoid failures. Thus, the characterization of materials and the processes going on in them is of considerable interest for the design of components to operate them safely and reliably. Aperiodic thermal-wave imaging methodology has been signifying as a consistent material characterization capability. In this work, a linear frequency modulated thermal wave imaging technique is applied in visualizing inclusions present in modeled mild steel sample. Also, an algorithm for automated defect identification is proposed for analyzing image contents, such as locating centers edges or regions and segmentation from the background image. Obtained results clearly show the capabilities of the proposed scheme for automatic detection of sub-surface defects. The shape of all the defects is recognized accurately irrespective of the type of inclusion used. It clearly distinguishes the elliptical irregular defects (for all defects, different materials are used for inclusions) present in the metallic sample from the sample's sound regions and gives the other geometrical parameters of detected anomalies.
11.	Digitized frequency modulated thermal wave imaging for defect estimation in steel **A Rani, P Mishra**, V Arora, **R Sekhar**, R Mulaveesala - Advances in Non Destructive Evaluation (NDE, 2021): Conference Proceedings, 2024 **Abstract:** Active InfraRed Thermography (IRT) have gained wide acceptance in the field of Non-Destructive Testing and Evaluation (NDT&E) due to fast, non-contact and wide area inspection supported by various modulated excitation schemes. This paper introduces a novel analytical model for sub-surface defect detection using Digitized Frequency Modulated Thermal Wave Imaging (DFMTWI) technique. The applicability of the proposed technique has been validated over a steel sample containing six square defects located at different depth locations. Further, the defect detection capability of the approach has been assessed by comparing the existing Frequency Domain (FD) and Time Domain (TD) data analysis approach.
12.	Economic and feasibility study of biomass-based electric power generation

	R Goswami, R Das, S Ganguly - AIP Conference Proceedings, 2024 **Abstract:** In this paper, the gasification of blue gum (Eucalyptus globulus) biomass is carried out in a 10 kW downdraft gasifier system (power plant) to generate electric power. Further, the potential capability of different biomass for energy production and the trend of electricity demand in India are highlighted in order to frame the significance of biomass resources to fulfill the energy demand, especially in developing countries. The main portion of the work includes an economic analysis of biomass gasification-based power generation plants for various capacities (10 kW, 500 kW, and 1000 kW) under the present scenario of India. It has been revealed that the capital cost per kW diminishes as we increase the capacity of the plant. The electricity production costs of 10 kW, 500 kW, and 1000 kW are estimated as Rs.9.57/kWh (0.120 USD/kWh), Rs.4.65/kWh (0.058 USD/kWh) and Rs.4.34/kWh (0.055 USD/kWh), respectively. Although the electricity production cost for small capacity power plants is high with respect to the current grid supply, it is economically sustainable compared to the diesel power plant that has an electricity production cost of Rs.14.44/kWh (0.181 USD/kWh). The minimum payback period is found as 3.12 years for 1000 kW capacity power. The outcomes of this research will be helpful in conveying the viability, selection, and installation of a biomass-based power plant.
13.	Experimental analysis of digitized frequency modulated thermal wave imaging for non-destructive testing and evaluation of materials **J Kaur, A Rani, R Sekhar**, R Mulaveesala - Advances in Non Destructive Evaluation (NDE, 2021): Conference Proceedings, 2024 **Abstract:** Thermal Wave Imaging (TWI) has gained wide acceptance in the field of Non-Destructive Testing and Evaluation (NDT&E) due to its reliable, remote, fast and quantitative characterization of various materials such as semiconductors, metals, composites, etc. The present work highlights the effectiveness of Digitized Frequency Modulated Thermal Wave Imaging (DFMTWI) technique for detection of sub-surface defects in a specimen. The capability of the proposed technique has been compared with the popular pulse based and mono-frequency thermal excitation schemes by carrying out an experimental study over a specimen containing Flat Bottom Hole (FBH) defects.
14.	FeaMod: Enhancing modularity, adaptability and code reuse in embedded software development M Al Maruf, A Azim, **N Auluck, M Sahi** - 2024 IEEE International Conference on Information Reuse and Integration (IRI), 2024 **Abstract:** The increasing prevalence of embedded systems in Cyber-Physical Systems (CPS) and the Internet of Things (IoT) has amplified the necessity for effective and adaptable software development practices. The challenges encountered in designing and developing these systems stem from the requirement to efficiently integrate advanced computational paradigms like machine learning and fog computing. Their inherent complexity and rigidity often limit the systems' adaptability to evolving requirements and complicate the effective management of feature dependencies, versioning, customization, and configuration in distributed environments. To address these challenges, we propose the FeaMod framework, integrating feature-based modularity with adaptive feature modeling for enhanced efficiency in embedded software design. Using the Bidirectional Encoder Representations from Transformers (BERT) model, FeaMod employs automated feature extraction through advanced static code analysis, facilitating the identification of computational features and requirements from existing codebases. These features are encapsulated in an adaptive feature model (AFM) that encourages code reuse and allows for dynamic configuration and system integration. By introducing a set of rules governing feature relationships, our approach ensures the adaptive nature of the model, enhancing its flexibility in response to changing system requirements, user preferences, and varying environmental conditions.

15.	Inspection of sub-surface defects using linear frequency modulated thermal wave imaging **A Rani**, S Singh, R Mulaveesala - Conference and Exhibition on Non Destructive Evaluation, 2021 **Abstract:** InfraRed Thermography (IRT) is an effective tool for Non-Destructive Testing and Evaluation (NDT&E) of structural components consisting of fiber reinforced polymers (FRP). Active thermography is a safe and reliable technique for health monitoring of these materials during in-service applications. The present work focuses on the defect depth resolvability in a carbon fiber reinforced polymer (CFRP) sample using frequency modulated thermal wave imaging (FMTWI) technique. The performance of the FMTWI has been explored using correlation-based pulse compression approach and compared with the conventional data processing approaches. Results shows the high sensitivity and resolution to resolve deeper defects of varying depths and diameters in CFRP sample using correlation approach.
16.	IoT-based wearable band for elderly care **A Phutela, SS Patare, S Pal** - 2024 IEEE 21st International Conference on Mobile Ad-Hoc and Smart Systems (MASS), 2024 **Abstract:** Healthcare for elderly is an important topic in the medical field. A lot of efforts in this direction have been made in the past to create various surveillance system for monitoring the health of the elderly. In this paper, we propose an enhanced healthcare monitoring system for elderly person based on non invasive sensors. We integrated multiple sensors for monitoring the health as well as location of any person at any give instant of time. Additionally, using this framework, the healthcare professionals and caregivers can receive the alert in case of emergency. This system will give timely intervention and safeguard elders who are at risk and require assistance.
17.	LS+: Informed label smoothing for improving calibration in medical image classification **AS Sambyal, U Niyaz, S Shrivastava**, NC Krishnan, **DR Bathula** - International Conference on Medical Image Computing and Computer-Assisted Intervention (MICCAI 2024), 2024 **Abstract:** Deep Neural Networks (DNNs) exhibit exceptional performance in various tasks; however, their susceptibility to miscalibration poses challenges in healthcare applications, impacting reliability and trustworthiness. Label smoothing, which prefers soft targets based on uniform distribution over labels, is a widely used strategy to improve model calibration. We propose an improved strategy, Label Smoothing Plus (LS+), which uses class-specific prior that is estimated from validation set to account for current model calibration level. We evaluate the effectiveness of our approach by comparing it with state-of-the-art methods on three benchmark medical imaging datasets, using two different architectures and several performance and calibration metrics for the classification task. Experimental results show notable reduction in calibration error metrics with nominal improvement in performance compared to other approaches, suggesting that our proposed method provides more reliable prediction probabilities. Code is available at https://github.com/abhisheksambyal/lsplus.
C	**Journal Article(s)**
18.	3D-CTM: Unsupervised crop type mapping based on 3-D convolutional autoencoder and satellite image time series **K Singh**, R Ranjan, **S Ghildiyal**, S Tamaskar, **N Goel** - IEEE Geoscience and Remote Sensing Letters, 2024 **Abstract:** Accurate and timely mapping of different crop types holds significant importance for food security and crop management at regional and global levels. This letter proposes a novel 3-D-crop type mapping (CTM) model based on an unsupervised crop-type mapping technique using satellite image time series (SITS) data and a 3-D convolutional autoencoder (CAE). The

	study uses a combination of five different vegetation indices: Normalized Difference Vegetation Index (NDVI), Red-Edge Chlorophyll Vegetation Index (RECl), Normalized Difference Red Edge Vegetation Index (NDRE), Green Normalized Difference Vegetation Index (GNDVI), and Visible Atmospherically Resistant Index (VARI) of time series data, along with a 3D-CAE for feature extraction. The model underwent evaluation employing one publicly accessible dataset and one in-house dataset sourced from the PlanetScope instruments. In the case of the in-house dataset, the model has achieved an accuracy of 88.75%, 73.88%, and 93.97% for maize, paddy, and sugarcane, respectively. In the case of the publicly available dataset, the model has achieved an accuracy of 83.71%, 72.81%, and 75.37% for paddy, triticale, and barley, respectively. Our 3D-CTM model demonstrates higher accuracy in mapping the crop types, which can be further utilized for effective management of the agricultural sectors.
19.	A classical thermodynamic model for dispersed nanophase stability and its application for investigating the stability of air nanobubbles in water **A Verma**, H Paliwal, **N Gopinathan** - Industrial & Engineering Chemistry Research, 2024 **Abstract:** There is a growing need to understand the theoretical basis of nanophase stability to enable the control and manipulation of their properties. Bulk nanobubbles are examples of dispersed nanophases that show promising properties for clean, green, sustainable, and yield enhancement applications. In this work, a chemical equilibrium thermodynamic framework is presented to study the nanophase. This framework is used to prove the spontaneity of nanobubble formation and thereby its stability through the estimation of the corresponding Gibbs energy. Estimation of bubble pressure, temperature, and internal gas composition is also carried out for a typical air–water nanobubble system by employing this framework. The work shows that the curved nanointerface is critical for nanobubble stability and also exhibits unusual characteristics as it traps gas molecules at extremely high pressures, ∼1100 atm, when the bulk pressure is just 1 atm, while maintaining high surface area and reactivity. We were able to thermodynamically and mathematically show the existence of very strong interactions at the nanobubble interface, the nature of which is assumed to be primarily Coulombic, but how the Coulombic forces form extremely strong molecular traps is still unknown. The existence of these interfacial interactions, i.e., their origin and nature, have to be explored experimentally. However, there are no probes that can measure the charge present on the Stern layer around a nanobubble as well as pressure, temperature, and composition inside a nanobubble dispersed in a bulk fluid. Thus, the development of new characterization techniques or an investigation using molecular simulation in the future could validate the estimates of nanobubble pressure, temperature, and composition, as well as the interfacial interactions estimated in this work. 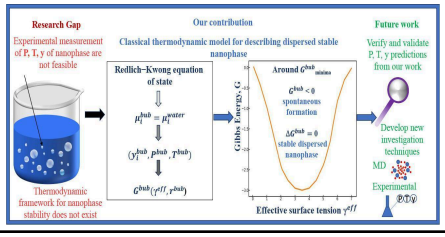
20.	A DT framework integrating human and artificial intelligence for power consumption prediction in CNC machining **A Pratap**, TK Vi, YW lee, **N Sardana**, PA Hsiung, YC Kao - The International Journal of Advanced Manufacturing Technology, 2024 **Abstract:** Digital twins (DT) have increasingly garnered attention in today's manufacturing industry for their potential to enhance productivity, efficiency, and decision-making processes. This study presents a human-centric digital twin framework (HCDT) specifically designed for a three-axis vertical milling machine (VMC3), following the ISO 23247 standard. Our system

	seeks to offer a comprehensive virtual depiction of a tangible milling machine, facilitating immediate monitoring, analysis, and enhancement of machining operations. This study targets specifically the prediction of power consumption in three-axis vertical machining using advanced machine learning. Power consumption during modified Kakino toolpath cutting was examined through a series of trials that involved adjusting spindle speed, depth of cut, and feed rate. The analysis was conducted utilizing physical sensors, mathematical modeling, and machine learning. The utilization of machine learning methods, specifically random forest, exhibited encouraging outcomes, as evidenced by a mean absolute error (MAE) of 17.30. In addition, virtual simulations were performed to forecast power usage. The proposed applied digital twin (ADT) incorporates human intelligence and artificial intelligence to effectively integrate physical and virtual environments, offering a unique approach that adheres to the ISO 23247 framework. The cross-system entity of the digital twin showcases that the calculated power has large variations with the experimental power. However, the proposed ADT approach has resulted in higher similarity to the calculated, experimental, and predicted power consumption respectively in the proposed digital twin scenario. Also, the addition of explainability to the result has developed the trustworthiness in the digital twin environment.
21.	A miniaturized coupler-integrated rectenna element to eliminate hybrid-coupler circuit for polarization insensitive wireless power transmission **VK Malav, A Sharma** - IEEE Transactions on Microwave Theory and Techniques, 2024 **Abstract:** In wireless power transfer (WPT), rectenna is utilized to wirelessly charge the Internet of Things (IoT) nodes. The harvesting performance of the rectenna depends on the wave polarization; thus, a polarization-insensitive (PoI) rectenna is desired to allow free rotation of the IoT nodes. Typically, a dual linearly polarized (DLP) antenna is employed for this, and to achieve full PoI, the prior arts emphasize the necessity to insert a hybrid coupler (HC) between the rectifiers and the DLP antenna. However, the use of complex circuits, i.e., HC, matching networks (MNs), and rectifiers, degrades the power conversion efficiency (PCE) and increases rectenna size. Therefore, in this article, a new rectenna system is analytically evolved having an HC-like feature to achieve PoI without employing an HC circuit. Hence, a fully integrated dual circularly polarized rectenna (DCPR) is proposed which simultaneously achieves the desired PoI performance together with enhanced PCE and miniaturization. The proposed design was experimentally validated. The results show a 126% enhancement in PCE by the proposed DCPR over the conventional HC-based rectenna where both achieve PoI and the former is miniaturized. Hence, the proposed DCPR is a good rectenna contender for wireless charging of randomly oriented miniature IoT nodes.
22.	A new minimum DC voltage ripple generating PWM selection algorithm for voltage source inverter **AI Gedam, KR Sekhar, N Kumar** - IEEE Journal of Emerging and Selected Topics in Power Electronics, 2024 **Abstract:** The voltage source inverters (VSIs) generate the average output voltage using the instantaneous switching voltage vector. The difference between the average output voltage and instantaneous switching voltage vector produces the error voltage, contributing to DC voltage ripple and DC source current ripple. In this work, a novel minimum DC voltage ripple generating PWM selection algorithm is proposed for three phase two level voltage source inverter. To elicit the minimum DC voltage ripple, firstly, the DC capacitor current, DC voltage ripple and DC source current ripple are mathematically modeled for a three-phase two-level VSI using an error voltage vector approach. Based on mathematical modeling, different continuous PWM (CPWM) and discontinuous PWMs (DPWMs) are compared to derive the minimum DC voltage ripple. After comparison, the minimum DC voltage ripple regions is identified for CPWMs and DPWMs in modulation index (ma) and load angle (δ) plane. Based on the identified regions, an adaptive switching PWM selection algorithm is proposed to ensure the minimum DC voltage ripple

	irrespective of the load operating conditions. The proposed method of selecting minimum voltage ripple yield PWMs is demonstrated on experimental prototype by implementing PWMs on DSP C2000 TMS320F28379D board.
23.	An investigation of the formability of ultra-thin CP-Ti-Gr2 foils considering thickness-to-grain-size effects under controlled heat treatment in μ-ISF **M Pal, A Agrawal, CK Nirala** - Journal of Manufacturing Processes, 2024 **Abstract:** Micro-forming is an emerging micro-manufacturing process for the fabrication of miniature parts/components made of ultra-thin sheets (foils), forged billets, rods, etc. Achieving high formability in the micro-incremental sheet forming (μISF) process is difficult due to the size-effect and non-optimal selection of process parameters viz. step depth (Δz). The major sources of size-effects are pure volume source, surface-to-volume ratio, thickness-to-grain-size (t/d ratio), surface structure scalability, etc. In the micro-scale processes, studying the grain size of the material is crucial to understand the deformation behaviour. Additionally, the anisotropy is very prominent in thin foils and affects the micro-forming process adversely. In the present work, the intrinsic anisotropy of the foils is minimized through controlled heat treatment, and varying grain sizes, having different microstructures, are generated to investigate their effect on the formability of CP-Ti-Gr2 foils. Initially, the properties of the received material are tested along different directions through the uniaxial tensile test, followed by furnace annealing to produce equiaxed recrystallized grains and reduce the anisotropy of the foils. Subsequently, the specimens are heat-treated at different temperatures to generate a wide spectrum of grain sizes. Through extensive μISF experiments, it was established that higher annealing temperature and increase in grain size assisted in improving the ductility of the foils, leading to enhanced formability. Therefore, the combined effect of the grain size and step depth on the formability of the components is investigated. A relationship between formability and t/d ratio was established and its critical value was obtained. Interesting observations, contrary to those in macro-ISF process were observed, e.g. higher step depth in μISF helped in improving the formability of the micro-parts. The results were confirmed by measuring the forming forces during the process, and it presented a strong correlation with the yield stress values, further correlated with varying grain sizes of the foil. This work could pave the way for designing the μISF process parameters considering the size-effects at micro-scale deformation, through optimum t/d ratio, for maximizing the formability. 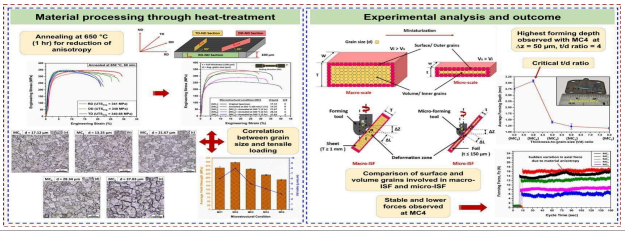
24.	Bandgap formation mechanism in tacticity inspired elastic mechanical metastructures A Dwivedi, **RK Munian**, B Bhattacharya, S Adhikari - Scientific Reports, 2024 **Abstract:** Tacticity is long known as a significant contributor in changing the chemical and mechanical properties of the polymers drastically. This study explores mechanism of bandgap formation in elastic mechanical metastructures designed with a focus on tacticity. We introduce metabeams, comprising a primary slender beam embedded with short secondary beams featuring end masses at their tips. The investigation delves into the numerically simulated vibration characteristics of metabeams using finite element analysis, with a subsequent comparison to experimental results for fabricated metabeams. Employing a unit-cell design approach that manipulates spatial and physical parameters, we explore a wide range of uniform and non-uniform metabeam configurations based on the distance between secondary beams and distribution of local resonators as per tacticity. Hence, drawing inspiration from tacticity, we

	extend our investigation to isotactic and syndiotactic metabeams, altering physical parameters (mass) within the unit cell for both configurations. The strategic distribution of end masses on attached secondary beams introduces unique characteristics to isotactic and syndiotactic metabeams, allowing for the modulation of bandgaps without altering the natural frequencies of the resonators in symmetric and anti-symmetric metabeam designs. Our research demonstrates, incorporating tacticity in metabeam design offers a novel and unconventional approach to modulate the bandgap formation mechanism.
25.	Bayesian neural networks modeling for tool wear prediction in milling Al 6061 T6 under MQL conditions J Airao, **A Gupta, CK Nirala**, AWJ Hsue - The International Journal of Advanced Manufacturing Technology, 2024 **Abstract:** The integration of artificial intelligence, machine learning, and deep learning algorithms into machining processes has made them more intelligent, significantly reducing costs, improving production rates, and enhancing product quality by accurately predicting machining responses. In this study, a Bayesian neural network (BNN) is employed to predict tool wear during the milling of Al6061 T6 alloy, showcasing the novelty of BNN in handling uncertainty and providing reliable predictions. Milling experiments were conducted at three different spindle speeds under dry, flood, and minimum quantity lubrication (MQL) strategies. Machinability was evaluated by considering tool wear, milling forces, and surface quality. Unique to this study is the use of force and current signals as input to the BNN model, capturing real-time data to estimate tool wear. The signals were trained and tested to predict tool wear under varying cutting conditions. The results indicated that tool wear in dry conditions was primarily due to adhesion, leading to higher milling forces and poorer surface quality. In comparison, the wet and MQL conditions resulted in 11–21% and 9–13% less tool wear, respectively, than dry conditions, alongside improved surface roughness and reduced machining forces. The BNN model demonstrated its ability to avoid overfitting, providing highly accurate predictions with an error margin of 2–15% when compared to experimental results. Unlike conventional models, the BNN accounts for prediction uncertainty, making it more robust and reliable across different datasets. Thus, the proposed BNN model proves its effectiveness and generalizability in predicting tool wear under various machining conditions, setting a new benchmark for the application of artificial intelligence in machining processes.
26.	Designing lotus-like superhydrophobic self-cleaning surface using carbon nanotubes **S Rahal**, MD Choudhury, SK Das, **D Samanta, PK Agnihotri** - Physics of Fluids, 2024 **Abstract:** Artificial superhydrophobic and self-cleaning surfaces are desirable in many engineering applications. Lotus leaves have long been the benchmark for the design and fabrication of artificial non-wetting surfaces. Here, we report the design and fabrication of superhydrophobic surfaces that mimic the behavior of lotus leaves. Akin to the microstructure of lotus leaves, an intrinsically hierarchical microstructure is created using carbon nanotubes (CNTs). The conventional CNT growth protocol is modified to induce multiscale features with lower diameter CNTs on the top of thicker CNTs. Together they form a dandelion seed head type structure with thicker CNTs such as “beak” and thinner CNTs such as “pappus.” The wetting and self-cleaning behavior of the CNT coated surface is compared with the lotus leaves. The wetting behavior of never-wet commercial spray and Cu and Ni foils are also recorded for comparison. The contact angle, contact angle hysteresis, and sliding angle of water drops on CNT coated surface are comparable with the lotus leaves. The wobbling motion of water drops on the CNT coated surface is similar to that on the lotus leaves and spray coated surface with varying contact line length with time. It also induces the self-cleaning characteristics of CNT coated surfaces similar to lotus leaves. Finally, the present study demonstrates a feasible strategy to design and fabricate lotus leaves like artificial superhydrophobic surfaces with hierarchical CNT structures.

27.	Effect of prevalent irregular configuration of infills on the seismic collapse of Indian RC buildings **PL Kurmi, P Haldar** - Structure and Infrastructure Engineering, 2024 **Abstract:** Rapid urbanization and land scarcity obligated the urban population for multi-use of Reinforced Concrete (RC) buildings to meet both residential and commercial purposes together. Un-Reinforced Masonry (URM) infills are often placed irregularly in plan and or elevation of the buildings in some floor(s), particularly in the ground floor to suit the need of occupational requirements accompanied by the inherent irregularities due to openings for doors and windows to meet functional requirements for residence. Seismic performance of infilled frame highly depends upon degree of infill-frame interaction, and it is of utmost importance to classify infilled frame buildings in various Model Building Types (MBTs) based on the type of irregular placement of infills in addition to the parameters affecting seismic performance. Based on field pilot surveys carried out in Indian cities, URM infilled buildings have been classified into 14 different MBTs. Seismic performance of the prevalent categories of MBTs have been evaluated through Incremental Dynamic Analysis (IDA). It has been observed that irregular placement of infills increases the seismic collapse risk significantly, and reduces collapse capacity to approximately 50% as compared to ideal uniformly infilled building. Global collapse occurred due to failure of structural members in the vicinity of irregularity created due to infills.
28.	Effect of Zn addition on phase evolution in AlCrFeCoNiZn high-entropy alloy **V Shivam, D Beniwal**…**PK Ray**, NK Mukhopadhyay - Advanced Engineering Materials, 2024 **Abstract:** The addition of Zn to AlCrFeCoNi high-entropy alloy (HEA) poses intriguing questions as to how it would affect phase evolution. Herein, the phase evolution in AlCrFeCoNiZn is studied using a combination of experimental techniques (X-ray diffraction, scanning electron microscopy, energy-dispersive spectroscopy, and differential scanning calorimetry) and computational (density-functional theory [DFT], calculation of phase diagrams, and machine-learning) methods. Mechanically alloyed and spark-plasma-sintered AlCrFeCoNiZn assumes a metastable single-phase, body-centered-cubic (BCC) structure that undergoes diffusion-controlled phase separation upon subsequent heat treatment to form separate (Al, Cr)-rich, (Fe, Co)-rich, and (Zn, Ni)-rich phases. The formation of (Al, Cr)-rich phase, not reported previously in AlCrFeCoNi-based HEAs, is attributed to strong clustering tendency of Cr–Zn and Cr–Ni pairs, combined with the strong ordering of Zn–Ni pair, driving out Cr that in turn combines with Al to form a (Al, Cr)-rich phase. In the DFT results, the formation of thermodynamically stable L12 phase is shown wherein Cr–Fe–Zn [Al–Ni-Co] preferably occupy1a (000) [3c (0 ½ ½)] positions. The sluggish diffusional transformation to L12 phase from BCC precursors is attributed to the small stacking-fault energy of AlCrFeCoNiZn. The equilibrated HEA exhibits a high microhardness of 8.24 GPa with an elastic modulus of 184 GPa.
29.	Electronic, optical and thermoelectric behavior of KCuX (X = S, Se, Te) monolayers N Gupta, S Kumar, S Rani, P Kumari, S Kar, **R Ahuja**, SJ Ray - Journal of Physics: Condensed Matter, 2024 **Abstract:** In the past few decades, two-dimensional materials gained huge deliberation due to their outstanding electronic and heat transport properties. These materials have effective applications in many areas such as photodetectors, battery electrodes, thermoelectrics, etc. In this work, we have calculated structural, electronic, optical, and thermoelectric (TE) properties of KCuX (X = S, Se, Te) monolayers (MLs) with the help of first-principles-based calculations and semi-classical Boltzmann transport equation. The phonon dispersion calculations demonstrate the dynamical stability of the KCuX (X = S, Se, Te) MLs. Our results show that the MLs of KCuX (X = S, Se, Te) are semiconductors with band gaps of 0.193 eV, 0.26 eV, and 1.001 eV respectively, and therefore they are suitable for photovoltaic applications. The optical analysis illustrates that the maximum absorption peaks of the KCuX (X = S, Se, Te) MLs are located in the visible and ultraviolet regions, which may serve as a promising candidate for designing advanced optoelectronic devices. Furthermore, thermoelectric properties of the KCuS and

	KCuSe MLs, including Seebeck coefficient, electrical conductivity, electronic thermal conductivity, power factor and figure of merit are calculated at different temperatures of 300 K, 600 K, and 800 K. Additionally, we also focus on the analysis of Grüneisen parameter and various scattering rates to further explain their ultra-low thermal conductivity. Our results show that KCuS and KCuSe possess ultra-low lattice thermal conductivity value of 0.15 $Wm^{-1}K^{-1}$ and 0.06 $Wm^{-1}K^{-1}$ respectively, which is lower than those of recently reported KAgSe (0.26 $Wm^{-1}K^{-1}$ at 300 K) and TlCuSe (0.44 $Wm^{-1}K^{-1}$ at 300 K), indicating towards the large value of ZT. These materials are found to possess desirable thermoelectric and optical properties, making them suitable candidates for efficient thermoelectric and optoelectronic device applications.
30.	Enhanced corrosion protection performance using polysilazane-derived amorphous SiCN ceramic coating **R Bura, Vishnu GC, RM Prasad** - Surface and Coatings Technology, 2024 **Abstract:** In this work, a polymer-derived silicon carbonitride (SiCN) ceramic layer has been deposited on stainless steel 304 (SS304) to enhance the corrosion resistance of SS304 in a seawater environment. SS304 is dip-coated with a polysilazane solution followed by pyrolysis under argon environment at 800 °C to develop SiCN ceramic layer with a thickness of about 3 μm on SS304. Structural characterization of the prepared samples was performed using Fourier transform infrared (FTIR), X-ray diffraction (XRD), Raman spectroscopy, and scanning electron microscopy (SEM). Potentiodynamic polarization tests of SS304 and SiCN-coated SS304 were performed in 0.6 M NaCl solution. SiCN-coated SS304 showed very low corrosion current density of 4.2×10^{-10} A/cm^2 whereas corrosion current density of uncoated SS304 was measured to be 1.52×10^{-7} A/cm^2. Excellent corrosion resistance performance of SiCN-coated SS304 was observed as confirmed by electrochemical impedance spectroscopic (EIS) measurements.
31.	Excitation of high-quality quasi-BIC toroidal mode in a lattice perturbed terahertz metasurface BK Bhowmik, KM Rohith, **P Duhan**, G Kumar - Applied Physics Letters, 2024 **Abstract:** The bound state in continuum (BIC) is a phenomenon that describes the existence of nonradiative modes (dark modes) embedded in the continuum frequency range. However, an ideal BIC cannot be detected experimentally. The BIC can be transformed into a quasi-BIC by establishing a leaky channel to the radiation continuum. In this study, instead of the conventional asymmetric split ring resonator structure, a sharp quasi-BIC mode is excited in a symmetric split ring resonator (SRR) metasurface by the perturbation of the lattice constant of the unit cell via changing the interspacing distance between two adjacent SRRs. The quality factor of the quasi-BIC mode can be tuned by varying the interspacing of two SRRs, while the resonance frequency of the quasi-BIC mode remains stable. An eigenmode analysis confirms the presence of the quasi-BIC mode, while the ab initio Fano theory and a coupled oscillator model elucidate the radiative and nonradiative coupling mechanisms. The influence of geometric perturbations on the quasi-BIC mode is quantitatively assessed through the extracted fitting parameters, providing insights into the transition from the dark mode (ideal BIC) to the quasi-BIC mode. The terahertz time domain spectroscopy measurement demonstrates a signature of the quasi-BIC resonance mode as a result of the band folding in the first Brillouin zone induced by the doubling of the lattice constant.
32.	Experimental investigation of heat transfer coefficient and frictional pressure drop in flow boiling of R513A: Comparative analysis of micro-fin and smooth tubes NK Vidhyarthi, **S Deb**, S Pal, AK Das - Proceedings of the Institution of Mechanical Engineers, Part E: Journal of Process Mechanical Engineering, 2024 **Abstract:** The heat transfer coefficient (HTC) and frictional pressure drop (FPD) of R513A in flow boiling conditions experimentally investigated in the present article. The study employed

	micro-fin tubes (MFT1 and MFT2) and smooth tubes (ST1 and ST2) as testing tubes under various operational parameters. The test sections featured standardized tube lengths (1000 mm) and outer diameter (9.52 mm) across all tubes, with variations in mass flux (50–300 $kg \cdot m^{-2} \cdot s^{-1}$), vapor quality (0.02–0.96), saturation temperature (12°C, 17°C, and 22 °C) and heat flux (6, 18, and 30 $kW \cdot m^{-2}$). Research focused on evaluating influence of micro-fin enhancement on flow boiling characteristics, specifically comparing HTC and FPD between micro-fin and smooth tubes. Results indicate significant improvement on HTC within micro-fin tubes compared to smooth tubes, accompanied by reasonable increase in FPD. Additionally, the study validated experimental data against established correlations and conducted sensitivity analysis to understand influence of key parameters on HTC and FPD. Overall, findings contribute valuable insights for optimizing heat exchanger design and thermal system efficiency in flow boiling applications.
33.	Exploring N-centered umpolung reactivity in photoredox-catalyzed amidation with an α-iminoester **P Mistry, S Das, R Patra, I Chatterjee** - Organic Chemistry Frontiers, 2024 **Abstract:** The synthesis of amides and their derivatives has gained significant attention from the scientific community in recent decades due to the presence of amide moieties in many bioactive organic molecules. Pursuing sustainable chemistry using cost-effective starting materials under mild reaction conditions is intriguing and challenging. In this context, we present a method for the direct synthesis of amides from α-keto acids and α-iminoesters. This approach employs an Ir-based photocatalyst to enable redox-neutral C–N bond formation at room temperature through N-center umpolung chemistry. This straightforward protocol is compatible with a broad range of functional groups, allowing for the efficient production of amides from aromatic keto acids and imines as coupling partners in an atom-economical manner.
34.	Fluorescent ionic liquid aggregates: A self-assembled approach for pesticide detection and catalysis **T Akhtar, K Kaur, G Singh**, N Kaur, **N Singh** - Journal of Agricultural and Food Chemistry, 2024 **Abstract:** The unregulated use of pesticides, industrial discharge of heavy metals, waste, and agricultural runoff may contaminate surface water and groundwater, consequently threatening ecosystems and human health. Thus, the sensitive detection and degradation of pesticides are essential for safety. In this context, herein, we have developed benzimidazolium-based fluorescent surfactant assemblies **TA-1/SDS** and **TA-2/SDBS**, which exhibit aggregation-induced emission enhancement in an aqueous medium. The aggregates (**TA-1/SDS** and **TA-2/SDBS**) displayed a turn-on emission response upon interaction with carbendazim and azamethiphos with limits of detection 7.5 and 7.8 nM, respectively. The FE-SEM and AFM studies revealed that **TA-1/SDS** and **TA-2/SDBS** undergo self-assembly with the addition of AZA and CBZ, resulting in the formation of dendritic structures. In addition to the quantification of AZA and CBZ, **TA-1/SDS** and **TA-2/SDBS** have also been evaluated to degrade both pesticides and validated using ^{31}P NMR spectroscopy and LC-MS spectrometry. 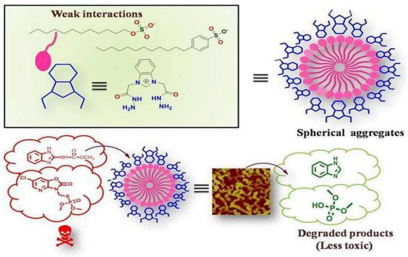
35.	Generating optical vortex needle beams with a flat diffractive lens **A Kumari, V Dev**, TM Hayward, R Menon, **V Pal** - Journal of Applied Physics, 2024

	Abstract: We present a novel method for generating optical vortex needle beams (focused optical vortices with extended depth-of-focus) using a compact flat multilevel diffractive lens (MDL). Our experiments demonstrate that the MDL can produce focused optical vortices (FOVs) with topological charges l=1-4 (extendable to other l values), maintaining focus over distances significantly longer than conventional optical vortices. Specifically, FOVs exhibit non-diffracting behavior with a depth-of-focus (DOF) extended beyond 5 cm, compared to conventional optical vortices, which show continuous size increase due to diffraction. When the MDL is illuminated by an optical vortex of 3 mm diameter, it achieves a transmission efficiency of approximately 90% and extends the DOF several times beyond that of traditional lenses. Increasing the size of the input optical vortex further extends the DOF but introduces additional rings, with their number increasing proportionally to the value of l. Our approach, validated by both experimental results and numerical simulations, proves effective for beams such as optical vortex and Hermite-Gaussian modes and holds potential applications in high-resolution imaging, material processing, optical coherence tomography, and three-dimensional optical tweezers, offering a simple and efficient solution for generating non-diffracting beams.
36.	Hydrostatic and chemical pressure driven crossover from the commensurate to the incommensurate state of the Weyl semimetal Mn3+x Sn1-x K Bhattacharya, AK Bharatwaj, C Singh, **R Gupta**, R Khasanov, S Kanungo, AK Nayak, M Majumder - Physical Review B, 2024 **Abstract:** The observation of large intrinsic anomalous Hall conductivity (AHC) in the noncollinear antiferromagnetic phase of the Weyl semimetal Mn3Sn generates enormous interest in uncovering the entanglement between the real-space magnetic ordering and the momentum-space band structure. Previous studies show that changes in the magnetic structure induced by the application of hydrostatic and chemical pressure can significantly affect the AHC of the Mn3+xSn1-x system. Here, we employ the muon spin relaxation/rotation (μ+SR) technique to systematically investigate the evolution of different magnetic states in the Mn3+xSn1-x as a function of hydrostatic and chemical pressure. We find two muon sites experimentally, which is also supported by our ab initio calculations. Our μ+SR experiments affirm that the x=0.05 compound exhibits a commensurate magnetic state throughout the magnetically ordered phase below the Neel temperature TN≈420 K in ambient pressure. In contrast, we observe an incommensurate magnetic state below TIC∼175 K when a hydrostatic pressure of 1.5 GPa is applied. A similar transition from the commensurate to incommensurate state is also found with chemical pressure for x=0.04 and x=0.03, using μ+SR and elastic neutron scattering experiments. Using band structure calculations, we have shown the emergence of Fermi nesting in Mn3Sn and the subsequent development of incommensurate magnetic ordering under hydrostatic/chemical pressure.
37.	Impact of pollutants on groundwater quality and health risk assessment of quaternary aquifers in Northern India A Gani, A Hussain, **S Pathak…** - Journal of Hazardous, Toxic, and Radioactive Waste, 2025

	Abstract: The tremendous increase in the population and the establishment of numerous industrial setups in the last few decades has caused an augmentation in the demand for water. This has led to a greater reliance on groundwater instead of surface water resources. Due to the dumping of vast industrial effluents and other anthropogenic activities, groundwater quality has worsened. The purpose of this study was to develop the water quality indices to categorize the groundwater quality of the holy city of Mathura, Uttar Pradesh, India. To depict the quality of water for various geographic locations in the city, GIS mapping has been carried out. In addition, to evaluate the impact of groundwater pollution on human health in the city, a health risk assessment has been carried out using the assessed physicochemical parameters. The results during the premonsoon season indicate that out of 75 sampling locations, four sampling location samples were poor, 34 sampling locations had very poor quality water, and the water from the remaining 37 sampling sites was unacceptable for drinking consumption. However, during the postmonsoon season, out of the 75 sampling locations, nine were of poor quality water; in 35 sampling locations, the water was of very poor quality, and the water in the remaining 31 locations was unsuitable for drinking. The result for cancer risks (CRs) indicates that during the premonsoon season, there is a higher risk of cancer for infants and children, but infants are more prone than children. However, in the postmonsoon season, infants and children are susceptible to carcinogenic diseases, but infants are more prone than children during this season. Therefore, the water indices and health risk assessment that were developed in this study could be utilized by researchers and policymakers in the overall planning and management of groundwater pollution and could be helpful for the safeguarding of society.
38.	Influence of dissolved organic matter on U(VI) removal at varying hydrogeochemical scenarios in ultrafiltration process **M Verma, VA Loganathan** - Separation and Purification Technology, 2025 **Abstract:** Uranium (U) is a chemical and radioactive groundwater contaminant that needs to be regulated in drinking water to avoid health hazards. In this study, we have investigated the mechanisms underlying ultrafiltration (UF) process, a low energy-intensive technology, for the removal of uranium from contaminated groundwater, in the presence of dissolved organic matter (i.e. Humic Acid [HA]) under environmentally-relevant conditions representative of regional scenario of Punjab, India. Stirred cell UF experiments with aqueous solutions containing uranium were performed with five different UF membranes with molecular weight cut off (MWCO) ranging from 1 kDa to 30 kDa at a pH of 8.5 that represented ambient groundwater scenario. In the absence of HA, the U(VI) removal was highest for the UF membrane with the lowest MWCO (i.e. 1 kDa) and vice-versa. Further, the effect of various solution parameters viz. pH, concentration of HA, and salinity have been studied using three different UF membranes viz. 5 kDa, 10 kDa, and 30 kDa. Uranium rejection was found to be maximum at pH 5.5 with ca. 97 %, 94 %, and 87 % rejection for 5 kDa, 10 kDa, and 30 kDa membranes, respectively. Further, U(VI) speciation results of the hydrogeochemical model corroborated that the removal of U(VI) in the presence of HA was highly dependent on feed solution pH. Moreover, U(VI) removal increased significantly with an increase in HA concentration, indicating the dominant role of U(VI)-HA complexes. Further, it was observed that increasing the salinity levels to 100 mM in the feed solution (i.e. semi-brackish water scenario) decreased U(VI) rejection primarily due to the charge screening effect. Our results show that using the UF separation process, the World Health Organization's drinking water guideline value of 30 µg of U L^{-1} could be achieved in U(VI) contaminated groundwater that contains significant HA levels.

	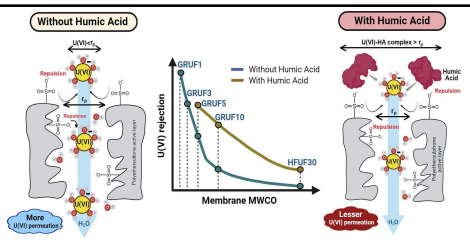
39.	Instability dynamics of viscous fingering interaction on dual displacement fronts A Patmonoaji, Y Nagatsu, **M Mishra** - Journal of Fluid Mechanics, 2024 **Abstract:** We explored the instability dynamics of the viscous fingering interaction in dual displacement fronts by varying the viscosity configuration. Four regimes of rear-dominated fingering, front-dominated fingering, dual fingering and stable were identified. By using the breakthrough time, which refers to the breakup of the dual displacement fronts, the instability dynamics were modelled, and a regime map was developed. These serve as a tool for effectively harnessing the dual displacement fronts for various applications, such as hydrogeology, petroleum, chemical processes and microfluidics.
40.	Inverse problem assisted multivariate geostatistical model for identification of transmissivity fields **A Kapoor**, D Kashyap - Frontiers in Water, 2024 **Abstract:** Groundwater models often require transmissivity (T) fields as an input. These T fields are commonly generated by performing univariate interpolation of the T data. This T data is derived from pumping tests and is generally limited due to the large costs and logistical requirements. Hence T fields generated using this limited data may not be representative for a whole study region. Groundwater models often require transmissivity (T) fields as an input. These T fields are commonly generated by performing univariate interpolation (using kriging, IDW etc.) of the T data. This T data is derived from pumping tests and is generally limited due to the large costs and logistical requirements. Hence, the T fields generated using this limited data may not be representative for the whole study region. This study presents a novel cokriging based methodology to generate credible T fields. Cokriging - a multivariate geostatistical interpolation method permits incorporation of additional correlated auxiliary variables for the generation of enhanced fields. Here abundantly available litholog derived saturated thickness data has been used as secondary (auxiliary) data given its correlation with the primary T data. Additionally, the proposed methodology addresses two operational problems of traditional cokriging procedure. The first operational problem is the poor estimation of variogram and cross-variogram parameters due to sparse T data. The second problem is the determination of relative contributions of primary and secondary variable in the estimation process. These two problems have been resolved by proposing a set of novel non-bias conditions, and linking the interpolator with a head based inverse problem solution for credible estimation of these parameters. The proposed methodology has been applied to Bist doab region in Punjab (India). Additionally, base line studies have been performed to elucidate the superiority of the proposed cokriging based methodology over kriging in terms of head reproducibility.
41.	Investigating the feasibility of agro-waste briquettes as a sustainable energy source in Borno state Nigeria as pathways for post-conflict and instability recovery **SA Waziri**, K Singh, UA Maina… - Discover Sustainability, 2024 **Abstract:** The growing energy demand and lack of access to clean energy sources call for the development of more energy for cooking in households, briquettes produced using agricultural materials and related biomass have the capacity for utilization as an energy source. This study aims to introduce briquettes as an alternative energy source for cooking within conflict-affected communities in Borno State, northeastern Nigeria, where factors relating to the high cost of

	charcoal, security constraints, and the environmental impact of tree cutting have sparked apprehension and raised concerns. The study demonstrates the likelihood of adopting briquettes as a cooking fuel alternative in communities recovering from insurgency. Using assessment tools such as household surveys, Key Informant Interviews (KIIs), and Focus Group Discussions (FGDs), involving a total of 536 questionnaires administered to respondents; KII was administered to 37 respondents and 9 FGDs with cooperatives and dealers in traditional fuel were conducted. From the results 73% of the community relies on charcoal as their primary fuel source, since the majority (68.7%) appeared to be low-income households, 24.1% reported that the high cost of charcoal is a major hindrance to continued usage. However, despite the communities showing potential in briquettes, only 3.7% are aware of briquettes as an alternative option for cooking energy indicating the adoption of briquettes being low in the region. A situational assessment was carried and sensitization strategies were recommended as means to enhance livelihoods and build resilience within the community.
42.	Kerr beam self-cleaning under different initial modal excitation conditions in the anomalous dispersion regime of a graded-index multimode fiber **LK Sharma, V Pal** - Optical Fiber Technology, 2024 **Abstract:** We investigated the phenomenon of Kerr beam self-cleaning (KBSC) under a variety of initial modal excitation conditions in the anomalous dispersion region of a graded-index multimode fiber (GRIN-MMF) by solving the generalized multimode nonlinear Schrodinger equation (GMMNLSE). Our results clearly indicate that the phenomenon of beam self-cleaning is highly dependent on the initial modal excitation conditions, and the power threshold (P_{th}) required for beam self-cleanup varies depending on the initial modal energy distribution conditions considered. We also show that such beam self-cleanup does not occur for any arbitrary initial modal excitation, even at the highest values of input power launched. The temporal and spectral analysis reveals that a spatiotemporal soliton formed initially at a certain power value becomes unstable, thereby shedding dispersive waves and a number of multimode solitons through the fission process, and the nonlinear energy exchanges among the constituent modes lead to a self-cleaned multimode beam. Moreover, we also show that the use of the fiber of longer length permits us to substantially reduce the power threshold (P_{th}) required to observe beam self-cleaning. Our results realizing the Kerr beam self-cleaning effect with femtosecond pulses in the anomalous dispersion regime of a GRIN-MMF offer innovative and interesting perspectives for the potential extension of the concept of thermalization of classical nonlinear waves to the spatiotemporal domain and may pave the way for a better understanding and control of various novel nonlinear spatiotemporal phenomena in multimode platforms, in developing the next generation of tunable, broadband high-power lasers with nearly single-mode emission.
43.	LINC01116-dependent upregulation of RNA polymerase I transcription drives oncogenic phenotypes in lung adenocarcinoma **SS Sarkar, M Sharma, S Saproo, S Naidu** - Journal of Translational Medicine, 2024 **Abstract:** Background: Hyperactive RNA Polymerase I (Pol I) transcription is canonical in cancer, associated with malignant proliferation, poor prognosis, epithelial-mesenchymal transition, and chemotherapy resistance. Despite its significance, the molecular mechanisms underlying Pol I hyperactivity remain unclear. This study aims to elucidate the role of long noncoding RNAs (lncRNAs) in regulating Pol I transcription in lung adenocarcinoma (LUAD). Methods: Bioinformatics analyses were applied to identify lncRNAs interacting with Pol I transcriptional machinery. Fluorescence in situ hybridization was employed to examine the nucleolar localization of candidate lncRNA in LUAD cells. RNA immunoprecipitation assay validated the interaction between candidate lncRNA and Pol I components. Chromatin isolation by RNA purification and Chromatin Immunoprecipitation (ChIP) were utilized to confirm the interactions of candidate lncRNA with Pol I transcriptional machinery and the rDNA core promoter. Functional analyses, including lncRNA knock-in and knockdown, inhibition of Pol I

	transcription, quantitative PCR, cell proliferation, clonogenicity, apoptosis, cell cycle, wound-healing, and invasion assays, were performed to determine the effect of candidate lncRNA on Pol I transcription and associated malignant phenotypes in LUAD cells. ChIP assays and luminometry were used to investigate the transcriptional regulation of the candidate lncRNA. Results: We demonstrate that oncogenic LINC01116 scaffolds essential Pol I transcription factors TAF1A and TAF1D, to the ribosomal DNA promoter, and upregulate Pol I transcription. Crucially, LINC01116-driven Pol I transcription activation is essential for its oncogenic activities. Inhibition of Pol I transcription abrogated LINC01116-induced oncogenic phenotypes, including increased proliferation, cell cycle progression, clonogenicity, reduced apoptosis, increased migration and invasion, and drug sensitivity. Conversely, LINC01116 knockdown reversed these effects. Additionally, we show that LINC01116 upregulation in LUAD is driven by the oncogene c-Myc, a known Pol I transcription activator, indicating a functional regulatory feedback loop within the c-Myc-LINC01116-Pol I transcription axis. Conclusion: Collectively, our findings reveal, for the first time, that LINC01116 enhances Pol I transcription by scaffolding essential transcription factors to the ribosomal DNA promoter, thereby driving oncogenic activities in LUAD. We propose the c-Myc-LINC01116-Pol I axis as a critical oncogenic pathway and a potential therapeutic target for modulating Pol I transcription in LUAD. 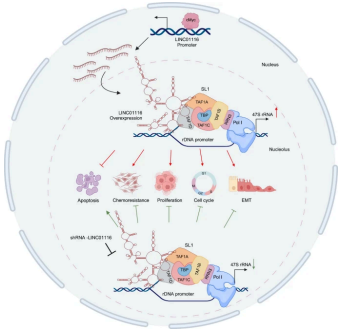
44.	Multifaceted analysis of microplastic pollution dynamics in the Yamuna River: Assessing anthropogenic impacts and ecological consequences **VS Pawak**, VK Bhatt, **M Sabapathy, VA Loganathan** - Journal of Hazardous Materials, 2024 **Abstract:** Microplastics (MPs) are pervasive contaminants that pose significant ecological and human health risks, emerging as one of the most widespread anthropogenic pollutants in natural environments. This study investigates the abundance, characteristics, and distribution of microplastics (MPs) in the Yamuna River, encompassing 29 sampling points across urban, rural, and industrial zones in and around Delhi, Mathura, Haryana, and Agra. Microplastics were identified and quantified using Nile red dye staining and Micro-Raman spectroscopy, with particle size distribution predominantly between 2 μm to 80 μm and the largest detected particle measuring 256.5 μm. The average MPs concentration was 14,717 ± 4444 L^{-1}, with a significant abundance of hazardous polymers such as polyethylene terephthalate (PET), polypropylene (PP), and polystyrene (PS). The study found that MPs were predominantly fragments and films (65.6 %) and fibers (30.6 %), with transparent particles being the most prevalent. The Pollution Load Index (PLI) consistently indicated high-risk levels (PLI > 100) at all sampling sites, highlighting substantial MP contamination. These results underscore the urgent need for continuous monitoring and the development of robust management strategies to address microplastic pollution in the Yamuna River. This study provides valuable insights into MPs spatial distribution and persistence, contributing to an improved understanding of their environmental impacts and guiding future mitigation and regulatory efforts.

	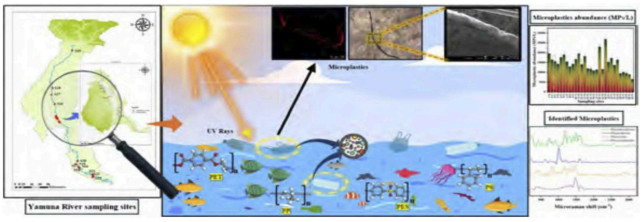
45.	Natural radioactivity in rocks and soil along Manali-Leh highway: comparative analysis J Yadav, …**PP Singh**… R Dalal - Journal of Radioanalytical and Nuclear Chemistry, 2024 **Abstract:** This study compares the concentration of naturally occurring radionuclides in rocks and soil samples taken along the Manali-Leh highway from the Higher and Tethyn Himalayas. The activity of ^{226}Ra, ^{232}Th, and ^{40}K in soil and rock samples was measured using an HPGe detector. The activity of these primordial radionuclides in soil and rocks differs considerably due to variations in geological and tectonic formations in the region. After a particular location, a significant decrease in radioactivity concentration in rocks and soil was also observed.
46.	N-Doped carbon nitride with embedded Pd nanoparticles for selective photocatalytic valorisation of biomass-derived vanillin into vanillyl alcohol and 2-methoxy-4-methyl phenol **H Dhiman, R Ghalta**, R Bal, **R Srivastava** - ACS Applied Nano Materials, 2024 **Abstract:** Efficient conversion of abundant biomass into high-value chemicals is crucial for sustainable chemical production. Herein, we report the design and synthesis of a Pd nanoparticles (NPs)-embedded N-doped carbon nitride (Pd@NCN) nanocomposite for the photocatalytic transformation of biomass-derived compounds. N-doping of carbon nitride using DMF significantly enhanced visible light absorption, as evidenced by DRUV spectroscopy, making it a suitable photocatalyst for blue LED-driven reactions. Subsequent decoration with Pd NPs remarkably improved the catalyst's performance. UPS measurements revealed that Pd NPs, with their lower Fermi level and higher work function compared to the photoactive support, act as efficient electron acceptors, promoting charge separation and improving the catalytic activity. This was corroborated by PL, TCSPC, and EIS studies. Photogenerated electrons on the Pd NPs surface-activated hydrogen, enabling the hydrogenation of biomass derivatives at room temperature. Concurrently, photogenerated holes were consumed by IPA via O–H and C–H, leading to acetone formation. The optimized 1% Pd@N0.75CN catalyst exhibited exceptional activity in the hydrogenation of vanillin (VAN), achieving 79.6% conversion and 94.4% selectivity to vanillyl alcohol (VOL) within an hour. Moreover, reaction selectivity could be tuned by adjusting Pd NPs loading and reaction time, leading to complete VAN conversion and excellent selectivity (~99%) to 2-methoxy-4-methylphenol (MMP) using 2% Pd@N0.75CN in 4.5 h. Comprehensive characterization and mechanistic studies provided insights into the structure–activity relationship, paving the way for the development of advanced NPs-based photocatalysts for challenging biomass valorization at ambient conditions. 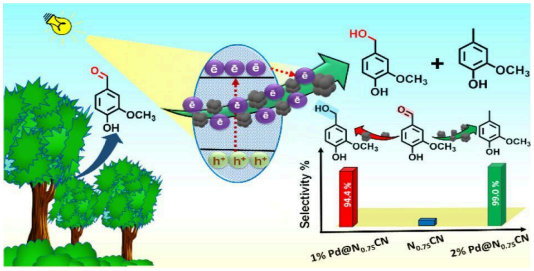
47.	Non-noble metal anchored 2D covalent organic framework for ambient CO2 fixation to high-value compounds **V Parihar, G Singh, N Duhan, S Kumar, TJD Kumar, CM Nagaraja** - ChemSusChem, 2024

	Abstract: The catalytic functionalization of CO2 into high-value compounds comprises a promising approach to mitigate its atmospheric content and sustainable generation of fine chemicals. Herein, we report application of a crystalline, nano-porous 2D COF (ET-BP-COF) for utilization of CO2. The ET-BP-COF features a unique 2D kagome (kgm) topology composed of hexagonal and triangular 1D channels decorated with bipyridine sites, which were exploited for covalent anchoring of eco-friendly Cu(I) by post-synthetic method. The Cu(I) engrafted COF was applied as a recyclable catalyst for coupling CO2 with alkynes to generate two high-value compounds, α-alkylidene cyclic carbonates (α-ACCs) and 2-oxazolidinones. Notably, Cu(I)@ET-BP-COF demonstrated excellent catalytic performance for transforming propargylic amine and CO2 to 2-oxazolidinone, an essential building block for antibiotics. Besides, an efficient transformation of propargylic alcohols to generate α-ACCs, valuable commodity chemicals, has been achieved by utilizing carbon dioxide. Further, detailed theoretical simulations disclosed the insight mechanistic path of Cu(I) catalyzed coupling of CO2 with alkynes to produce 2-oxazolidinones and α-ACCs. Significantly, Cu(I)@COF was reusable for multiple cycles without losing framework rigidity and catalytic performance. This study showcases the potential application of ET-BP-COF for stable anchoring of eco-friendly metals as catalytic sites for effective utilization of CO2 to produce two high-value products.
48.	On the twisted group ring isomorphism problem for a class of groups S Hatui, **G Kaur**, S Sabnam - Journal of Algebra, 2024 **Abstract:** The twisted group ring isomorphism problem (TGRIP) is a variation of the classical group ring isomorphism problem. It asks whether the ring structure of the twisted group ring determines the group up to isomorphism. In this article, we study the TGRIP for direct product and central product of groups. We provide some criteria to answer the TGRIP for groups by answering the TGRIP for certain associated quotients. As an application of these results, we provide several examples. Finally, we answer the TGRIP for extra-special *p*-groups, and for all but five groups of order p^5, where $p \geq 5$ is prime.
49.	Oxygen nanobubbles halt tumor aggression and metastasis by inhibiting hypoxia-induced epithelial-to-mesenchymal transition in lung and mammary adenocarcinoma **K Bhavya, K Agarwal, D Negi**, K Niveria, **Y Singh…N Nirmalkar, D Pal** - ACS Applied Nano Materials, 2024 **Abstract:** The rapid proliferation of cancer cells creates a hypoxic microenvironment in solid tumors, driving aggressiveness through epithelial-to-mesenchymal transition (EMT), invasion, and migration, often leading to resistance to conventional chemotherapies. Delivering oxygen directly to the tumor site can address these challenges. Herein, we fabricated liposomal encapsulated oxygen nanobubbles (L-ONBs) with nanoscale size that exhibit enhanced stability and efficient oxygen release. Characterization revealed that the robust stability and negative surface charge of L-ONB particles prevent aggregation and facilitate passive targeting to tumor tissues due to the enhanced permeability and retention effect, thereby significantly reducing the aggressiveness of lung and breast tumors. Oxygen nanobubbles countered the hypoxia-induced EMT pathway by facilitating prolyl hydroxylation of hypoxia-inducible factor 1α, leading to its proteasomal degradation. This process resulted in the upregulation of epithelial marker E-cadherin and the downregulation of mesenchymal markers such as N-cadherin and vimentin, along with a significant decrease in transforming growth factor-β and vascular endothelial growth factor-A. Overall, our study elucidates the cellular mechanisms by which L-ONBs inhibit hypoxia-induced tumor aggressiveness, highlighting their potential as a promising therapeutic option for managing solid tumors.

	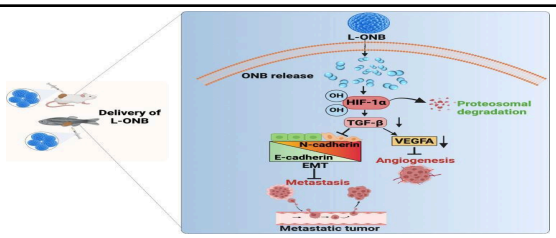
50.	Permafrost-induced hazard zonation using satellite data-driven multi-parametric approach employing AHP techniques in Alaknanda Valley, Uttarakhand, India T Ghosh, AC Pandey…**RK Tiwari** - Geo-information for Disaster Monitoring and Management, 2024 **Abstract:** Permafrost is one of the key components of the mountain cryosphere. An increase in global air temperature is leading to the melting of permafrost. Degradation and thawing of permafrost may induce multiple effects on the landscape, such as ground subsidence, increased frequency of landslides and rock falls due to destabilization of permafrost-covered slopes, further harming the infrastructures like roads, bridges, dams, buildings, etc. Climate models can predict further degradation of permafrost in the high mountain regions due to an increase in air temperature, resulting in changes in the terrestrial ecosystem and frequent permafrost-induced hazards. In the past decade, the area under investigation has experienced multiple natural hazards like slope failures, landslides, rock-ice avalanches, etc. In this study, assessment and hazard zonation of geohazards associated with mountain permafrost was attempted using AHP (Analytical Hierarchical Process) based multi-parametric approach. Based on its hazard susceptibility, the study area was categorized into three zones, namely, low, moderate, and high. Their corresponding area were 1738.28 km^2, 8945.77 km^2, and 518.89 km^2, respectively. The model output provided probable areas of hazard occurrence based on select topographical and climatic factors. Identifying regions with high hazard potential will help better understand the spatial distribution of such potentially hazardous sites within the study area, resulting in better mitigation and disaster management capabilities.
51.	Photoredox catalyzed reductive trifluoromethylation of imines via a radical umpolung strategy **H Paul, D Das, SK Ariyan, S Pradhan, I Chatterjee** - Chemical Communications, 2024 **Abstract:** Visible light-induced radical umpolung chemistry is utilized to synthesize trifluoromethylated unnatural α-amino acid and amine derivatives. This approach utilizes photoredox catalysis to perform a single-electron-transfer reduction of imines generating a N-centred radical that eventually migrates to the C-centre followed by a radical–radical cross-coupling to deliver reductive trifluoromethylation products.
52.	Predicting p53-dependent cell transitions from thermodynamic models **P Gautam**, I Ciuta, VB Teif, **SK Sinha** - The Journal of Chemical Physics, 2024 **Abstract:** A cell's fate involves transitions among its various states, each defined by a distinct gene expression profile governed by the topology of gene regulatory networks, which are affected by 3D genome organization. Here, we develop thermodynamic models to determine the fate of a malignant cell as governed by the tumor suppressor p53 signaling network, taking into account long-range chromatin interactions in the mean-field approximation. The tumor suppressor p53 responds to stress by selectively triggering one of the potential transcription programs that influence many layers of cell signaling. These range from p53 phosphorylation to modulation of its DNA binding affinity, phase separation phenomena, and internal connectivity among cell fate genes. We use the minimum free energy of the system as a fundamental property of biological networks that influences the connection between the gene network topology and the state of the cell. We constructed models based on network topology and equilibrium thermodynamics. Our modeling shows that the binding of phosphorylated p53 to promoters of

	target genes can have properties of a first order phase transition. We apply our model to cancer cell lines ranging from breast cancer (MCF-7), colon cancer (HCT116), and leukemia (K562), with each one characterized by a specific network topology that determines the cell fate. Our results clarify the biological relevance of these mechanisms and suggest that they represent flexible network designs for switching between developmental decisions.
53.	Probing NV center coupled metal-dielectric-metal architectures for quantum technologies **N Singh**, D Sehgal, A Venkatesan, **RV Nair** - Quantum 2.0, 2024 **Abstract:** We experimentally demonstrated the emission rate and intensity enhancement of NV centers mediated by metal-dielectric-metal cavity coupling. Results show the wide tunability of cavity mode, a vital platform for coupling various quantum emitters.
54.	Probing the influence of synthesized hierarchical ZSM-5 catalyst in ex-situ catalytic conversion of real-world plastic waste into aromatic rich liquid oil **Subhashini, T Mondal** - Journal of the Energy Institute, 2024 **Abstract:** Plastic waste management has become a vitally important environmental and economic concern for researchers and technologists worldwide. Currently, catalytic pyrolysis of plastic waste emerged as a promising plastic waste management technique, further aiding the full-scale development of an alternate innovation to convert plastic waste into fuel (liquid oil) energy. Lately, zeolites have been one of the most suitable and versatile catalysts in converting plastic waste into fuel grade hydrocarbons via catalytic pyrolysis. The present work exhibits an attempt to synthesize and study the performance of a hierarchical ZSM-5 in a fixed bed reactor to convert the real-world (LDPE, HDPE, PP and PS) plastic wastes into higher quality fuel grade liquid oil. The hierarchical ZSM-5 catalyst having both mesopores and micropores (dual porosity) in its framework is synthesized by using a single organic template i.e., 10 % tetra propylammonium hydroxide (TPAOH). The catalyst performance study displays remarkable selectivity and increase in the yield of the aromatic component in the liquid oil obtained from different plastic wastes. The results indicate that presence of hierarchical catalyst has exceptionally lowered the reaction temperature in the range of 400–430 °C and increased the liquid oil yield in comparison with that of the thermal pyrolysis. Also, the obtained liquid oils have comparable fuel properties with that of kerosene and diesel. 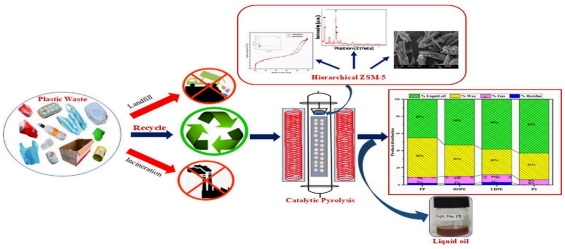
55.	Rapid detection of explicit volatile organic compounds for early diagnosis of lung cancer using MoSi2N4 monolayer T Hussain, P Panigrahi, Y Pal, **SP Kaur…** - Chemistry- An Asian Journal, 2024 **Abstract:** In this study, we investigate the adsorption of MoSi2N4) and MoSi2N4-VN towards five potential lung cancer volatile organic compounds (VOCs). Density functional theory calculations reveal that MoSi2N4 weakly adsorb the mentioned VOCs, whereas introduction of nitrogen vacancies significantly enhances the adsorption energies ([[EQUATION]]), both in gas phase and aqueous medium. The MoSi2N4-VN monolayers exhibit a reduced bandgap and facilitate charge transfer upon VOCs adsorption, resulting in enhanced [[EQUATION]] values of -0.83, -0.76, -0.49, -0.61, and -0.50 eV for 2,3,4-trimethyl hexane, 4-methyl octane, o-toluidine, Aniline, and Ethylbenzene, respectively. Bader charge analysis and spin-polarized density of states (SPDOS) elucidate the charge redistribution and hybridization between MoSi2N4-VN and the adsorbed VOCs. The work function of MoSi2N4-VN is significantly reduced upon VOCs

	adsorption due to induced dipole moments, enabling smooth charge transfer and selective VOCs sensing. Notably, MoSi2N4-VN monolayers exhibit sensor responses ranging from 16.2% to 26.6% towards the VOCs, with discernible selectivity. Importantly, the recovery times of the VOCs desorption is minimal, reinforcing the suitability of MoSi2N4-VN as a rapid, and reusable biosensor platform for efficient detection of lung cancer biomarkers. Thermodynamic analysis based on Langmuir adsorption model shows improved adsorption and detection capabilities MoSi2N4-VN under diverse operating conditions of temperatures and pressures.
56.	Real-time observation of stress-strain behavior beyond necking in martensitic steel by in-situ synchrotron X-ray diffraction **A Lavakumar**, S Hwang, K Okada… - ISIJ International, 2024 **Abstract:** In general, the stress-strain relationship of materials obtained by standard uniaxial tensile test, which can identify the hardening behavior only up to necking. Beyond necking, the material behavior is usually estimated by extrapolating or numerical modelling based on hardening behavior prior to the uniform elongation. This study investigated the post-necking hardening behavior of a fully martensitic steel by in-situ synchrotron X-ray diffraction during tensile deformation. From the in-situ results, the dislocation density, lattice strain and phase stress were calculated within the necked region and outside the necked region. A near steady-state flow with some hardening was observed within the necked region of a martensitic steel. However, beyond uniform elongation, outside the necked region the dislocation density and phase stress decreased slightly, suggesting stress relaxation. Steady-state flow and dislocation densities at large strains suggest dynamic recovery occurs in the martensitic steel at room temperature. 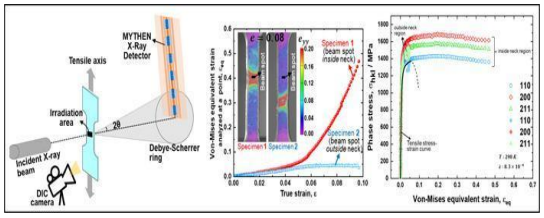
57.	Recycling valuable phenol from polycarbonate plastic waste via direct depolymerization and Csp2−Csp3 bond cleavage under mild conditions **AK Manal, D Rajendra Kanchan, A Banerjee**, J Zhao, **R Srivastava** - ChemSusChem, 2024 **Abstract:** Upcycling plastic waste into commodity chemicals is recognized as an environmentally benign solution and beneficial for the sustained growth of humanity. Nevertheless, transition metal-free catalysts and energy-efficient conditions pose significant challenges due to the robust mechanical properties of plastics. Here, a strategy for selective production of phenol by upcycling polycarbonate waste via direct depolymerization and Csp^2−Csp^3 bond cleavage in an aqueous medium under mild conditions is reported. The commercial zeolites efficiently catalyze the depolymerization, Csp^2−Csp^3 bond hydrolysis, and direct Csp^2−Csp^3 bond scission at Cα of PC. Among all evaluated zeolites, HY (*Si/Al*=15) showed excellent catalytic performance, attributed to the ~75 % yield of phenol and ~15 % of acetone. The approach also employs different municipal waste PC for upcycling. Studies reveal that HY (15) exhibits high catalytic efficiency and phenol yield due to its optimum acid sites and textual properties. A scale-up experiment demonstrated that 3.1 g of phenol was produced from 5.0 g of PC, and the mass balance was 90 %. A combination of control experiments, NMR analysis, and DFT studies proposed the reaction pathway. Our findings present a sustainable avenue for upcycling PC waste and offer a new way to produce phenol, contributing to the advancement of a circular economy.

	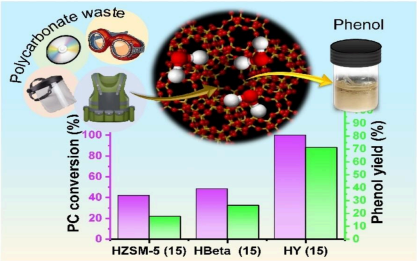
58.	Seasonal refuge patterns of phytoplankton trigger irregular bloom events in a contaminated environment **A Mandal**, S Biswas, PK Tiwari, S Pal - Scientific Reports, 2024 **Abstract:** Several experimental evidences and field data documented that zooplankton may alter its behavioral response in the presence of toxic phytoplankton, reducing its consumption to the point of starvation. This paper is devoted to the mathematical study of such interactions of toxic phytoplankton with grazer zooplankton. The non-toxic phytoplankton is assumed to adopt a density-dependent refuge strategy to avoid over-predation by zooplankton. Both groups of phytoplankton are assumed to suffer direct harm from anthropogenic toxicants, while zooplankton is affected indirectly by ingesting contaminated phytoplankton. We calibrate the proposed model with the field data from Talsari and Digha Mohana, India, and estimate some crucial model parameters consistent with the behavior of the observed data. Our results demonstrate that zooplankton grazing on toxic phytoplankton plays a key role in the emergence or mitigation of plankton blooms. We also highlight the system's potential to exhibit multiple stable configurations under the same ecological conditions. The plankton system experiences significant regime shifts, which are explored through various bifurcation scenarios, such as transcritical and saddle-node bifurcations. These shifts are influenced by changes in refuge capacity, species growth rates, and environmental carrying capacity. Furthermore, we incorporate environmental variations due to seasonal periodic or almost periodic changes, allowing the refuge parameter to be time-dependent. We observe that the forced system exhibits double periodic solutions. Moreover, stronger seasonal variations in the refuge pattern lead to irregular chaotic blooms. In conclusion, the results offer valuable insights into the sustainability of biodiversity, potentially shedding light on the origin of diverse plankton bloom phenomena.
59.	SWIPT module for battery less ultra low power sensor nodes **S Kumar**, V Sharma, **A Sharma** - IEEE Sensors Letters, 2024 **Abstract:** This letter proposes a simultaneous wireless information and power transfer (SWIPT) module capable of operating a battery-less ultra-low-power wireless sensor node (WSN). This module features a miniaturized circular patch antenna that utilizes a proximity-coupled feed to enable wireless information transfer (WIT) in the 5 GHz Wi-Fi band (5.15 GHz – 5.825 GHz). The WIT operation can be powered through wireless power transfer (WPT) to the proposed module using a capacitive coupled feed. The WPT is realized using a dedicated RF shower, which transmits RF energy in 4.9 GHz-5.1 GHz band. The different frequency bands are chosen for WIT and WPT to reduce the mutual coupling effect. Moreover, the use of orthogonal-polarized feeds for WIT and WPT further enhances the isolation between information and power signals. The design incorporates two conjugate matched shunt Schottky diodes, a stepped impedance low pass filter, and a parallel DC combining network for

	full-wave rectification (FWR) of the incident RF waves. Therefore, the proposed module ensures high power conversion efficiency (PCE) with a smaller footprint making it an ideal candidate for implementing battery-less WSN operation for IoT applications.
60.	Synergistic catalysis for promoting selective C–C/C–O cleavage in plastic waste: structure–activity relationship and rational design of heterogeneous catalysts for liquid hydrocarbon production **A Manal, A Shivhare**, S Lande, **R Srivastava** - Chemical Communications, 2024 **Abstract:** Ever-increasing consumption of plastic products and poor waste management infrastructure have resulted in a massive accumulation of plastic waste in environments, causing adverse effects on climate and living organisms. Although contributing ∼10% towards the total plastic waste management infrastructure, the chemical recycling of plastic waste is considered a viable option to valorize plastic waste into platform chemicals and liquid fuels. Among the various chemical upcycling processes, catalytic hydroprocessing has attracted interest due to its potential to offer higher selectivity than other thermal-based approaches. Heterogeneous catalytic hydroprocessing reactions offer routes for converting plastic waste into essential industrially important molecules. However, the functional group similarities in the plastic polymers frequently constrain reaction selectivity. Therefore, a fundamental understanding of metal selection for targeted bond activation and plastic interaction on solid surfaces is essential for catalyst design and reaction engineering. In this review, we critically assess the structure–activity relationship of catalysts used in the hydroprocessing of plastic waste for the selective production of liquid hydrocarbons. We discuss the significance of C–C/C–O bond activation in plastic waste through active site modulation and surface modification to elucidate reaction networks and pathways for achieving selective bond activation and cleavage. Finally, we highlight current challenges and future opportunities in catalyst design to upcycle real-life plastic waste and produce selective liquid hydrocarbons.
61.	Temperature-induced supersolidity in spin-orbit-coupled Bose gases **Rajat, Ritu**, A Roy, **S Gautam** - Physical Review A, 2024 **Abstract:** Close to the superfluid plane-wave (PW)–supersolid stripe (ST) phase transition point of a zero-temperature quasi-one-dimensional spin-orbit-coupled Bose gas, we find that an increase in temperature induces a phase transition to the supersolid phase with a broken translational symmetry from the superfluid plane-wave phase. We use the Hartree-Fock-Bogoliubov theory with the Popov approximation to investigate the effect of thermal fluctuations on the collective excitation spectrum and investigate the softening of the spin-dipole mode corresponding to the shift in the quantum critical point. This is in stark contrast to the PW-ST phase transition in a homogeneous system where nonzero temperatures facilitate the melting of the stripe phase.
62.	Tetrasubstituted chromanone synthesis by a tandem oxa-michael/michael addition reaction of 2-hydroxyacetophenones and alkynyl nitriles **C Kumari, NP Sahoo, M Kumar, A Goswami** - European Journal of Organic Chemistry, 2024 **Abstract:** An efficient transition metal-free approach for the synthesis of chroman-4-ones via double conjugate additions of 2-hydroxyacetophenones on alkynyl nitriles utilizing NaH as a base has been realized. This operationally simple protocol offers library of 4-chromanones in moderate to good yields.

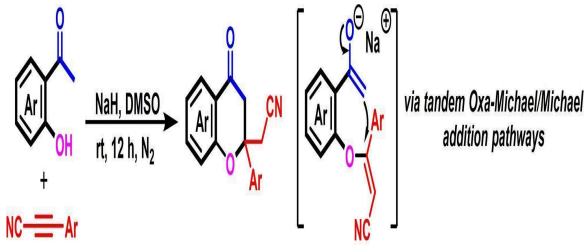

63.

[Tio2-decorated mos2 nanocomposite for co2 sensing at room temperature]
R Gond, P Shukla, B Rawat - IEEE Sensors Letters, 2024

Abstract: Continuous and real-time monitoring of CO_2 has become an urgent demand due to its significant impact on climate change, asphyxiation risks, agricultural productivity, and human health. Electrochemical sensors for CO_2 monitoring face challenges such as slow response time, high operating temperature, and lack of selectivity. To overcome these challenges, we propose a highly selective room-temperature (RT) CO_2 detection sensor based on TiO_2-MoS_2 nanocomposite, which is manufactured using a screen printing methodology. The fabricated sensor achieved a response of approximately 2.11% and response/recovery times of nearly 102/37 s at 1000 ppm. The sensitivity is observed to be approximately 0.0032%/ppm with an excellent response for the CO_2 concentration range of 500 to 5000 ppm. Despite the typically low selectivity of unreactive CO_2 gas, the fabricated sensor exhibits high selectivity, with a response of around 2.21× higher than that of the next CO gas with the highest response. The scalable fabrication methodology and RT operation make TiO_2-MoS_2 sensor a highly viable candidate for production through a cost-effective and high performance CO_2 sensing.

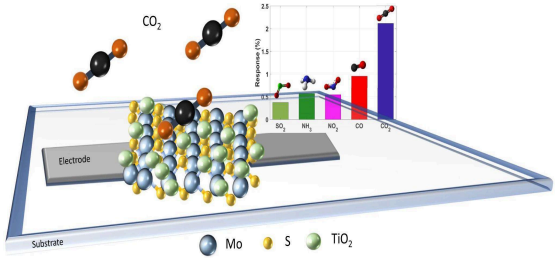

64.

[Traffic flow dynamics and oscillation control in conserved fractal networks]
M Verma, **AK Gupta**, S Sharma - The European Physical Journal B, 2024

Abstract: Traffic control serves as an indispensable component in optimizing the traffic flow, especially on networks. To analyze the varied complexity of traffic dynamics, the percolation backbone fractal network is characterized via cell-transmission model. Taking into account a generalized flow-density relation, dynamic model is modified to scrutinize the impact of transition rates on traffic flow in a conserved network. The macroscopic fundamental diagrams attained through numerical simulation are investigated for homogeneous as well as heterogeneous transition rates. For first-generation fractal network, unimodal or bimodal traffic currents are observed with respect to mean density. Further, for second-generation fractal network, two types of density waves are observed depending upon the number of vehicles present in system: uniform equilibrium state and oscillatory state. It is reported that the transition rates corresponding to singly connected nodes can control the traffic dynamics to ensure a uniform stationary flow, which cannot be achieved via the doubly connected and quadruple-connected nodes.

	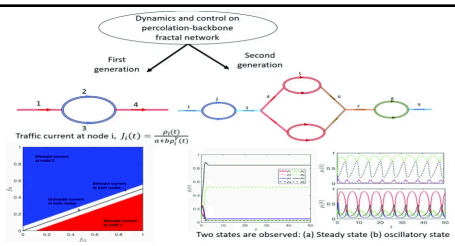
65.	Translating theoretical insights into an emotion regulation flexibility intervention: assessing effectiveness **P Sharma, P Singh** - Cognition and Emotion, 2024 **Abstract:** *Objective:* Traditional research often categorizes emotion regulation strategies as adaptive or maladaptive, overlooking crucial situational and individual differences that dictate their efficacy. The literature highlights the need for a more nuanced approach, like the role of emotion regulation flexibility. Despite its importance, research on developing and testing interventions that promote this flexibility is scarce. Addressing this gap, our study designed and tested an "Emotion Regulation Flexibility Booster Program" (ERFBP). We aimed to assess its efficacy in improving emotion regulation flexibility (ERF) and its impact on various mental health indicators. *Method:* We recruited 153 participants with low emotion regulation flexibility, randomly assigning them to experimental, control, and no-treatment groups. The experimental group was provided with an intervention based on an ERF model. The control group received sessions on study habits, whereas no-treatment group received no training. *Results:* The analysis indicated that participants in the ERFBP group exhibited significant changes in ERF, subjective wellbeing, and emotion regulation goals and psychological distress compared to baseline measurements and post-intervention scores of other two groups. *Conclusion:* These findings support the effectiveness of the ERFBP in enhancing ERF and wellbeing. However, further research must confirm these findings across diverse contexts and populations.
66.	WO_3 nanoparticle/biomass derived n-doped activated carbon decorated with polyaniline nanofibers ternary nanocomposite for high-performance symmetric and asymmetric supercapacitor D Bejjanki, M Mohan Seepana, **K Kumar**, S Kumar Puttapati - ChemistrySelect, 2024 **Abstract:** Supercapacitors have captured the curiosity of researchers due to their extremely high energy storage capacity. Hybrid supercapacitors deliver high specific capacitance values compared to the exciting (electrical double layer capacitor) EDLC and pseudocapacitors. This work presents a simple and scalable synthetic method to design a hybrid ternary composite as electrode material. In this work, the combination of EDLC-type behaviour material, i. e., sustainable biomass-derived Nitrogen-doped activated carbon (NAC) and pseudocapacitive behaviour electrode materials, i. e., metal oxides (tungsten oxide) and conductive polymer (polyaniline) are selected to achieve a high gravimetric capacity. The PANi/WO_3/NAC (PWNAC) ternary composite is tested for symmetric and asymmetric supercapacitor (ASC). In a symmetric capacitor, PWNAC acts as both the positive and negative electrode, whereas in ASC, PWNAC acts as the positive electrode and NAC as the negative electrode. It is observed that the ASC shows a better capacitance value than symmetric. ASC operates at a potential range of 1.4 V in 1 M H_2SO_4 aqueous electrolyte, shows a maximum capacitance of 608.2 F/g at 0.5 A/g, and has long capacitance retention of 98.32 % of its initial capacitance after 2000 charge-discharge cycles.

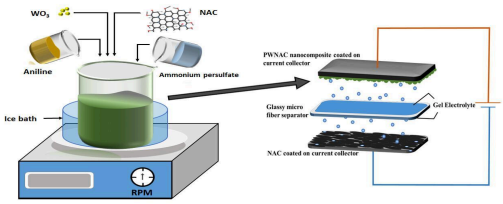

Disclaimer: This publication digest may not contain all the papers published. Library has compiled the publication data as per the alerts received from Scopus and Google Scholar for the affiliation “Indian Institute of Technology Ropar” for the month of October, 2024. The author(s) are requested to share their missing paper(s) details if any, for the inclusion in the next publication digest.